

***In silico* Exploration of some methyl 2-(4-(1H-pyrazol-5-ylamino)phenylthio)-1,2,3,4-tetrahydro-6-methylpyrimidine-5-carboxylate Derivatives to be developed as Potential EGFR inhibitors**

Sagar D. Magar^{1*}, Dr. Pratap Y. Pawar¹

¹Department of Pharmaceutical Chemistry, Dr. Vitthalrao Vikhe Patil Foundation's, College of Pharmacy, Ahmednagar, Maharashtra, 414111, India.

*Corresponding Author:

Email: sagarmagar2010@gmail.com; Orcid ID: <https://orcid.org/0000-0001-8467-849X>

Abstract

Many cancers' pathophysiology and progression correspond with EGFRs' high expression and/or adaptive activation, making them attractive targets for diagnostics and treatment. Various methods have been developed for inhibiting these receptors and/or EGFR-mediated actions in cancer cells. With the purpose of predicting the ADMET characteristics of compounds, a large number of *in silico* models have been constructed. However, it is still not easy to evaluate the drug-likeness of compounds in terms of so many ADMET properties. In present study, we have designed some methyl 2-(4-(1H-pyrazol-5-ylamino)phenylthio)-1,2,3,4-tetrahydro-6-methylpyrimidine-5-carboxylate derivatives to be developed as potential EGFR inhibitors for the treatment of cancer. The designed derivatives were screened through Lipinski rule, Veber's rule, ADMET analysis, drug-likeness properties and molecular docking. From above screening it was observed that native ligand formed three conventional hydrogen bonds and exhibited -8.3 kcal/mol binding affinity therefore, the molecules which formed three or more conventional hydrogen bonds and exhibited > -8.3 kcal/mol binding affinity with enzyme are considered as most potent and selected for wet lab synthesis followed by biological evaluation. Molecules **sm21**, **sm23**, **sm24**, **sm25**, **sm26**, **sm27**, **sm28**, **sm29**, and **sm36** had formed either three or more conventional hydrogen bonds with EGFR enzyme and hence selected for synthesis.

Keywords: EGFR, angiogenesis, cancer, ADMET, molecular docking

1. Introduction

Although radiation and chemotherapy may be used to treat a broad range of cancers, molecular targeting drugs can be more precisely directed at certain subtypes of tumors. Throughout the last several decades, researchers have made strides in understanding the interplay between cancer's cellular, metabolic, and genetic origins and development[1]. This newfound knowledge has led to the development of more tumor-specific anticancer therapies. Tyrosine kinases are often used as therapeutic targets because of their association with tumor formation and proliferation. Inhibitors of tyrosine kinases (TKIs) prohibit the related kinases from phosphorylating the tyrosine residues of their substrates, hence preventing the activation of downstream signaling cascades[2]. Over the last two decades, a number of robust and well-tolerated TKIs targeting single or multiple targets, such as EGFR, ALK, ROS1, HER2, NTRK, VEGFR, RET, MET, MEK, FGFR, PDGFR, and KIT, have been developed, advancing our understanding of precision cancer medicine based on a patient's genetic alteration profile[3]. The epidermal growth factor receptor (EGFR) has been identified as a molecular target for certain potential cancer therapies. Four transmembrane tyrosine kinases (EGFR1/ErbB1, Her2/ErbB2, Her3/ErbB3, and Her4/ErbB4), as well as thirteen secreted polypeptide ligands, make up the EGFR family[4]. Multiple solid tumours, including

breast, pancreatic, head and neck, kidney, vaginal, renal, colon, and non-small-cell lung cancer, have overexpressed EGFRs[5]. Overexpression of these genes causes cell proliferation, differentiation, cell cycle progression, angiogenesis, cell motility, and apoptosis inhibition through stimulating downstream signaling channels[6]. We will be able to quantify the individual activities of EGFR signalling networks as our understanding of their involvement in tumour activity advances. The high expression and/or adaptive activation of EGFRs correlates with the pathophysiology and progression of many cancers, making them attractive candidates for diagnostics and treatment. Several techniques have been developed to target these receptors and/or the EGFR-mediated effects in cancer cells. Monoclonal antibodies (mAbs) that specifically target the EGFR extracellular domain, such as cetuximab (Erbix), and small molecule TKIs that particularly target the EGFR catalytic domain, such as gefitinib (Iressa) and erlotinib(Tarceva), are two types of EGFRIs[7–11].

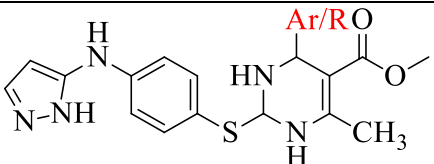
As a result, several computational models are built to predict the ADMET characteristics of compounds. Drug-likeness of compounds may be judged by their ADMET characteristics, however this evaluation is still challenging[12–19]. Here, we have carried out in silico ADMET screening of synthetic analogues that might be used as EGFR inhibitors in the future therapy of cancer. To determine which of the proposed compounds had the greatest potential as a medication, their ADMET profiles were analyzed computationally.

2. Material and Methods

2.1 Designing of methyl 2-(4-(1H-pyrazol-5-ylamino)phenylthio)-1,2,3,4-tetrahydro-6-methylpyrimidine-5-carboxylate derivatives

The structure of the parent compound and the substitutions of methyl 2-(4-(1H-pyrazol-5-ylamino)phenylthio)-1,2,3,4-tetrahydro-6-methylpyrimidine-5-carboxylate derivatives are depicted in Table 1.

Table 1. methyl 2-(4-(1H-pyrazol-5-ylamino)phenylthio)-1,2,3,4-tetrahydro-6-methylpyrimidine-5-carboxylate derivatives

			
Code	R/Ar	Code	R/Ar
Sm21	H	Sm31	—3-hydroxy phenyl
Sm22	—phenyl	Sm32	—2,3,4-trihydroxy phenyl
Sm23	—4-nitro phenyl	Sm33	—3-methoxy-4-hydroxy phenyl
Sm24	—4-bromo phenyl	Sm34	—2-methoxy phenyl
Sm25	—4-fluoro phenyl	Sm35	—4-styryl
Sm26	—4-chloro phenyl	Sm36	—naphthyl
Sm27	—4-methyl phenyl	Sm37	—2,4-dinitro phenyl
Sm28	—4-methoxy phenyl	Sm38	—4-methylsulfonyl phenyl
Sm29	—4-hydroxy phenyl	Sm39	—4-dimethylamino phenyl
Sm30	—3-nitro phenyl	Sm40	—4-trifluoromethyl phenyl

2.2 Pharmacokinetics and toxicity predictions of designed derivatives

Chemical absorption, distribution, metabolism, excretion, and toxicity (ADMET), play key roles in drug discovery and development. A high-quality drug candidate should not only have sufficient efficacy against the therapeutic target, but also show appropriate ADMET properties at a therapeutic dose. The

designed derivatives were screened for its ADME analysis, drug-likeness and toxicity parameters. The Lipinski rule of five and the pharmacokinetic (ADME) characteristics of designed derivatives were investigated using SwissADME[20] servers. The toxicity of the compounds has been predicted using ProTox-II, which is a freely accessible webserver for *in silico* toxicity predictions of new derivatives (http://tox.charite.de/prottox_II)[21].

2.3 Molecular Docking

All the selected compounds and the native ligand were docked against the crystal structure of the crystal Structure of EGFR T790M mutant in complex with naquotinib using Autodock vina 1.1.2 in PyRx 0.8[22]. ChemDraw Ultra 8.0 was used to draw the structures of the compounds and native ligand (mole. File format). All the ligands were subjected for energy minimization by applying Universal Force Field (UFF)[23]. The crystal structure of the enzyme with PDB ID 5Y9T was obtained from RCSB Protein Data Bank (PDB) (<https://www.rcsb.org/structure/5Y9T>). Discovery Studio Visualizer (version-19.1.0.18287) was used to refine the enzyme structure, purify it, and get it ready for docking[24]. A three-dimensional grid box (size_x=62.5293379415Å; size_y=43.0367205343Å; size_z=43.851824552Å) with an exhaustiveness value of 8 was created for molecular docking[22]. BIOVIA Discovery Studio Visualizer was used to locate the protein's active amino acid residues. The approach outlined by Khan et al. was used to perform the entire molecular docking procedure, identify cavity and active amino acid residues[12,13,15,17–19,25]. Fig. 1 shows the revealed cavity of enzyme with the native ligand molecule.

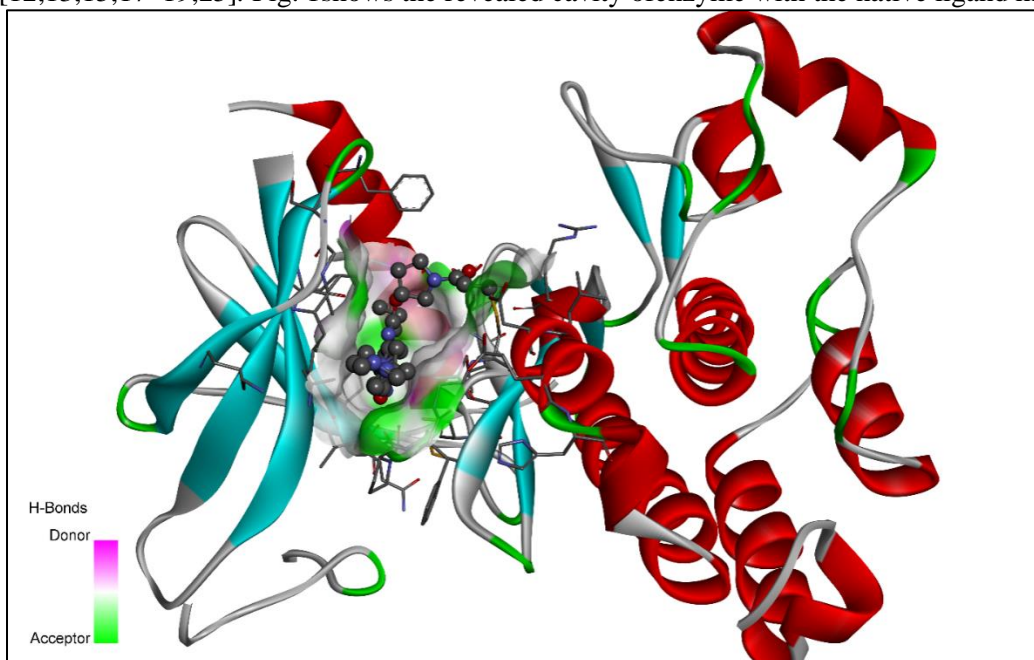


Fig. 1. The 3D ribbon view of the enzyme with native ligand in the cavity

3. Result & Discussion

Pharmacokinetic characteristics are critical to drug development because they enable scientists to investigate the biological impacts of possible pharmacological candidates[14]. This compound's oral bioavailability was evaluated using Lipinski's rule of five and Veber's rules (Table 2). To better understand the pharmacokinetics profiles and drug-likeness properties of the proposed compounds, the ADME characteristics of all of them were examined (Table 3). The oral acute toxicity have been predicted along with LD₅₀ (mg/kg), toxicity class, hepatotoxicity, carcinogenicity, immunotoxicity,

mutagenicity, and cytotoxicity (Table 4). Table 5 depicts the active amino residues, bond length, bond category, bond type, ligand energies, and docking scores. The docking poses of the molecules are exemplified in Table 6.

Table 2. Lipinski rule of 5 and Veber's rule calculated for molecules

Compound Codes	Lipinski rule of five					Veber's rule	
	Log P	Mol. Wt.	HBA	HBD	Violations	Total polar surface area (Å ²)	No. of rotatable bonds
NL	2.01	562.71	7	2	2	120.16	10
Sm21	1.92	345.42	4	4	0	116.37	6
Sm22	3.05	421.52	4	4	0	116.37	7
Sm23	2.49	938.71	4	4	1	116.37	8
Sm24	3.62	500.41	4	4	1	116.37	7
Sm25	3.37	439.51	5	4	0	116.37	7
Sm26	3.56	455.96	4	4	0	116.37	7
Sm27	3.39	435.54	4	4	0	116.37	7
Sm28	3.05	451.54	5	4	0	125.6	8
Sm29	2.66	437.51	5	5	0	136.6	7
Sm30	0.63	467.52	6	5	0	166.03	8
Sm31	2.67	437.51	5	5	0	136.6	7
Sm32	2.04	469.51	7	7	1	177.06	7
Sm33	2.72	467.54	6	5	0	145.83	8
Sm34	3.02	451.54	5	4	0	125.6	8
Sm35	3.84	461.58	4	4	0	116.37	9
Sm36	3.96	471.57	4	4	0	116.37	7
Sm37	-2.39	513.53	8	6	3	215.69	9
Sm38	2.75	499.61	6	4	0	158.89	8
Sm39	4.35	540.68	4	4	1	119.61	9
Sm40	5.39	565.61	7	4	2	116.37	9

Where: Mol. Wt., molecular weight; HBA, hydrogen bond acceptors; HBD, hydrogen bond donors.

Table 3. The pharmacokinetics and drug-likeness properties of developed compounds

Compound codes	Pharmacokinetics								Drug-likeness				
	GI abs.	BBB pen.	P-gp sub.	CYP1A2 inhibitors	CYP2C19	CYP2C9	CYP2D6	CYP3A4	Log K_p (skin permeation, cm/s)	Ghose	Egan	Muegge	Bioavailability Score
NL	H	N	Y	N	N	N	N	Y	-7.34	N	Y	Y	0.17
Sm21	High	No	Yes	Yes	No	No	No	No	-6.63	0	0	0	0.55
Sm22	High	No	Yes	No	Yes	Yes	Yes	Yes	-5.89	0	0	0	0.55
Sm23	High	No	Yes	No	No	No	No	Yes	-9.15	1	0	1	0.55
Sm24	High	No	No	Yes	Yes	Yes	No	Yes	-5.88	2	0	0	0.55
Sm25	High	No	Yes	Yes	Yes	Yes	No	Yes	-5.93	0	0	0	0.55
Sm26	High	No	Yes	Yes	Yes	Yes	No	Yes	-5.65	1	0	0	0.55
Sm27	High	No	Yes	No	Yes	Yes	No	Yes	-5.72	1	0	0	0.55
Sm28	High	No	Yes	No	Yes	Yes	Yes	Yes	-6.09	1	0	0	0.55
Sm29	High	No	Yes	No	No	Yes	No	Yes	-6.24	0	1	0	0.55
Sm30	Low	No	Yes	Yes	Yes	No	No	No	-6.62	1	1	1	0.55
Sm31	High	No	Yes	No	No	Yes	No	Yes	-6.24	0	1	0	0.55
Sm32	Low	No	No	No	No	No	No	No	-6.94	1	1	2	0.55
Sm33	Low	No	Yes	No	No	Yes	No	Yes	-6.45	1	1	0	0.55
Sm34	High	No	Yes	No	Yes	Yes	Yes	Yes	-6.09	1	0	0	0.55
Sm35	High	No	Yes	No	Yes	Yes	No	Yes	-5.47	1	0	1	0.55
Sm36	High	No	Yes	No	Yes	Yes	Yes	Yes	-5.31	1	0	1	0.55
Sm37	Low	No	Yes	No	No	No	No	No	-7.35	2	1	2	0.17
Sm38	Low	No	Yes	No	No	No	No	Yes	-6.91	2	1	1	0.55
Sm39	High	No	No	Yes	Yes	Yes	Yes	Yes	-5.37	3	0	1	0.55
Sm40	Low	No	No	Yes	No	No	Yes	Yes	-4.99	3	1	1	0.17

Where: NL, Native ligand; GI abs., gastrointestinal absorption; BBB pen., blood brain barrier penetration; P-gp sub., p-glycoprotein substrate

Table 4. The predicted acute toxicity of molecules

Compound codes	Parameters							
	LD ₅₀ (mg/kg)	Toxicity class	Prediction accuracy (%)	Hepatotoxicity (Probability)	Carcinogenicity (Probability)	Immunotoxicity (Probability)	Mutagenicity (Probability)	Cytotoxicity (Probability)
NL	800	4	23	I (0.60)	A (0.50)	A (0.80)	I (0.65)	I (0.71)
Sm21	1000	4	23	A (0.52)	A (0.56)	A (0.66)	I (0.58)	I (0.64)
Sm22	800	4	23	A (0.67)	A (0.56)	I (0.76)	I (0.61)	I (0.69)
Sm23	800	4	23	A (0.65)	A (0.50)	I (0.55)	I (0.61)	I (0.67)
Sm24	1700	4	23	A (0.69)	I (0.50)	A (0.72)	I (0.65)	I (0.65)
Sm25	1700	4	23	A (0.70)	I (0.50)	A (0.75)	I (0.65)	I (0.70)
Sm26	800	4	23	A (0.67)	I (0.50)	A (0.56)	I (0.66)	I (0.71)
Sm27	800	4	23	A (0.64)	A (0.54)	I (0.81)	I (0.61)	I (0.70)
Sm28	800	4	23	A (0.65)	A (0.52)	A (0.74)	I (0.57)	I (0.71)
Sm29	800	4	23	A (0.68)	A (0.57)	I (0.53)	I (0.57)	I (0.70)
Sm30	1000	4	54.26	A (0.68)	A (0.57)	I (0.53)	I (0.57)	I (0.70)
Sm31	800	4	23	A (0.68)	A (0.57)	A (0.83)	I (0.57)	I (0.70)
Sm32	1700	4	23	A (0.68)	A (0.55)	A (0.93)	I (0.56)	I (0.70)
Sm33	1700	4	23	A (0.65)	A (0.54)	A (0.97)	I (0.55)	I (0.72)
Sm34	730	4	23	A (0.65)	A (0.53)	A (0.89)	I (0.57)	I (0.72)
Sm35	1000	4	23	A (0.58)	A (0.55)	A (0.79)	I (0.58)	I (0.66)
Sm36	800	4	23	A (0.66)	A (0.55)	A (0.66)	I (0.59)	I (0.65)
Sm37	50	2	23	A (0.66)	A (0.55)	A (0.66)	I (0.59)	I (0.65)
Sm38	800	4	23	A (0.51)	I (0.50)	A (0.71)	I (0.68)	I (0.59)
Sm39	1700	4	23	A (0.57)	A (0.50)	A (0.81)	I (0.58)	I (0.69)
Sm40	1000	4	23	A (0.70)	A (0.51)	A (0.62)	I (0.65)	I (0.70)

Where: I, Inactive; A, Active

Table 5.The active amino residues, bond length, bond category, bond type, ligand energies, and docking scores

Active Amino acid	Bond length	Bond Type	Bond Category	Ligand Energy	Docking score
NL					
GLU758	3.88487	Electrostatic	Attractive Charge	568.59	-8.3
GLY857	2.87344	Hydrogen Bond	Conventional Hydrogen Bond		
GLU762	2.10926				
GLU758	3.35859				
GLU758	3.13642		Carbon Hydrogen Bond		
GLU758	3.33922	Electrostatic	Pi-Anion		
GLU762	3.56702				
ALA755	3.69661	Hydrophobic	Alkyl		
PRO877	4.97918				
Sm21					
LEU777	2.84453	Hydrogen Bond	Conventional Hydrogen Bond	400.36	-8.8
ALA1013	2.1967				
TYR1016	2.05493				
TYR1016	3.09459				
ASN700	2.21737				
GLN701	2.3989				
ARG776	4.87071	Electrostatic	Pi-Cation		
Sm22					
ASP837	2.13967	Hydrogen Bond	Conventional Hydrogen Bond	466.09	-7.3
ASN842	1.96901				
	3.80163	Hydrophobic	Pi-Sigma		
VAL726	3.83193				
PHE723	3.80781				
			Pi-Pi Stacked		
Sm23					
LEU718	2.2947	Hydrogen Bond	Conventional Hydrogen Bond	512.53	-8.9
ARG841	2.47205				
ASP855	2.41867				
ASP855	2.75915				
THR854	3.0971				
GLU762	2.34174				
ASP855	2.03631				
ASP855	4.13496	Electrostatic	Pi-Anion		

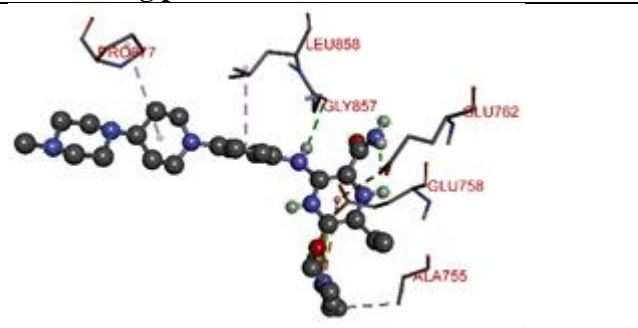
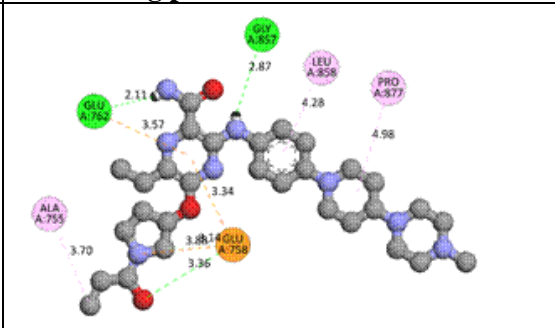
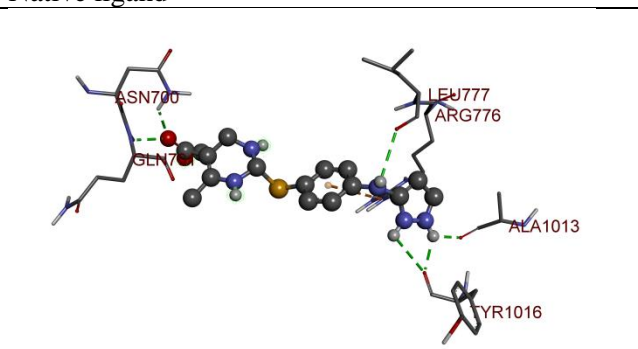
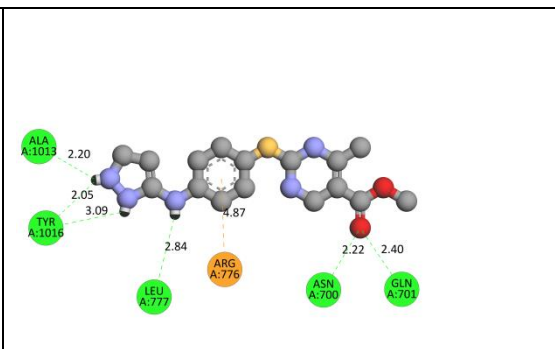
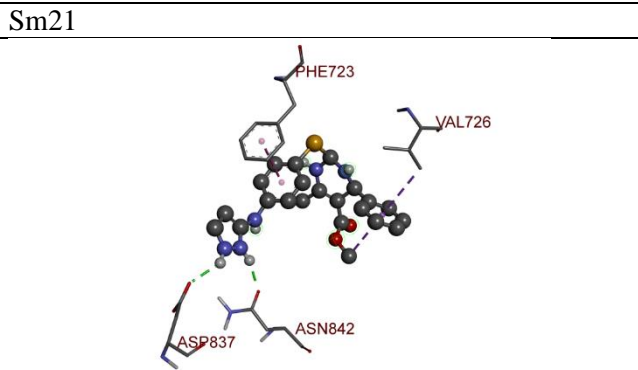
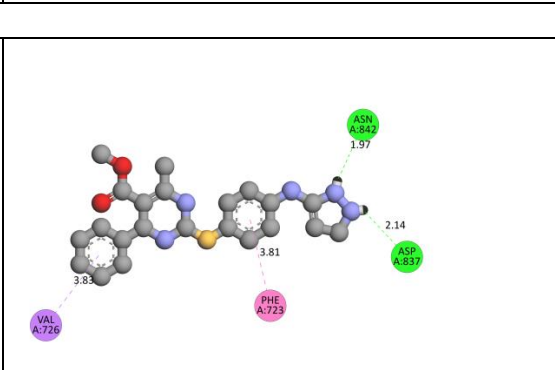
CYS797	3.88646	Hydrogen Bond;Other	Pi-Donor Hydrogen Bond;Pi-Sulfur		
PHE723	3.86852	Hydrophobic	Pi-Sigma		
VAL726	5.12492		Pi-Alkyl		
Sm24					
LEU718	2.57789	Hydrogen Bond	Conventional Hydrogen Bond	462.84	-8.5
PHE795	2.31553				
ASP800	2.82646				
PHE795	2.53146				
LEU718	3.81743	Hydrophobic	Pi-Sigma		
LEU844	3.9419				
CYS797	5.45415	Other	Pi-Sulfur		
	5.72658	Hydrophobic	Pi-Pi T-shaped		
LEU718	4.87159				
ALA743	3.8022				
LEU792	4.59763				
LEU844	5.33625				
VAL726	4.99547				
Sm25					
LEU718	2.63795	Hydrogen Bond	Conventional Hydrogen Bond	450.42	--8.3
ASP837	2.42677				
ASN842	2.66143				
ARG841	3.72735				
ASP855	3.68033				
	3.81738	Hydrophobic	Pi-Sigma		
VAL726	3.89061				
PHE723	3.88612				
LEU718	5.15463				
ALA743	5.23803				
LEU844	5.30021				
Sm26					
LEU718	2.57789	Hydrogen Bond	Conventional Hydrogen Bond	462.02	-8.5
PHE795	2.31553				
ASP800	2.82646				
PHE795	2.53146				
LEU718	3.81743	Hydrophobic	Pi-Sigma		

LEU844	3.9419				
CYS797	5.45415	Other	Pi-Sulfur		
	5.72658	Hydrophobic	Pi-Pi T-shaped		
LEU718	4.87159				
ALA743	3.8022				
LEU792	4.59763				
LEU844	5.33625				
VAL726	4.99547			Pi-Alkyl	
Sm27					
ALA1013	2.198	Hydrogen Bond	Conventional Hydrogen Bond	462.43	-8.3
TYR1016	2.37973				
LEU703	2.70171				
ILE1018	4.74365	Hydrophobic	Pi-Alkyl		
Sm28					
ALA767	2.85159	Hydrogen Bond	Conventional Hydrogen Bond	463.46	-8.8
LEU778	2.75924				
ALA1013	2.17243				
TYR1016	2.04226				
LEU703	2.38625				
ARG831	2.07794				
ILE1018	4.87483	Hydrophobic	Pi-Alkyl		
ALA702	5.41885				
Sm29					
ASP855	2.77914	Hydrogen Bond	Conventional Hydrogen Bond	466.92	-8.6
ASP837	2.33859				
ASN842	2.15216				
ASP855	2.56933				
THR854	1.8119				
GLY796	3.50176				
	5.07148	Hydrophobic	Pi-Pi T-shaped		
PHE723	5.03689				
LEU844	4.83446				Pi-Alkyl
Sm31					
ALA755	2.13354	Hydrogen Bond	Conventional Hydrogen Bond	444.21	-7.3
ARG836	2.20018				
LEU858	3.15591				

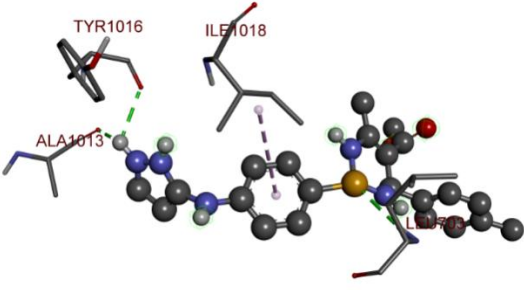
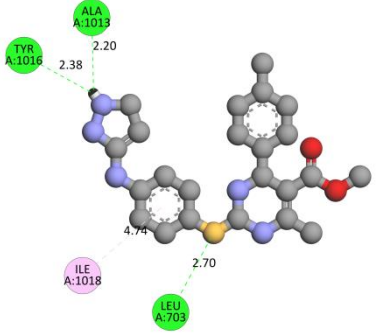
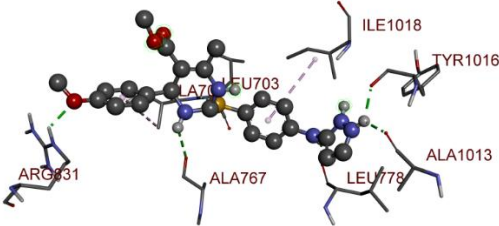
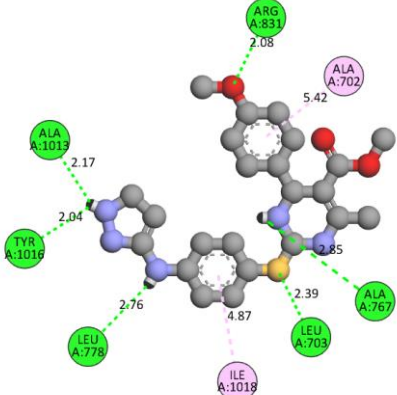
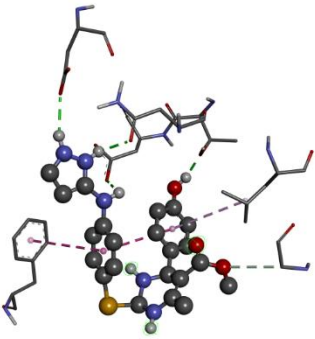
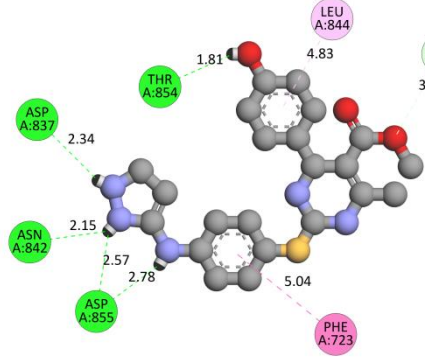
GLU758	3.68555	Electrostatic	Pi-Anion		
	3.57699	Hydrophobic	Pi-Sigma		
PHE723	4.26861		Pi-Pi Stacked		
Sm34					
GLN701	2.81436	Hydrogen Bond	Conventional Hydrogen Bond	497.63	-7.7
LEU703	3.45422		Carbon Hydrogen Bond		
MET766	3.56216				
ALA767	3.66227				
VAL769	3.52532				
LEU778	5.34385	Hydrophobic	Pi-Alkyl		
ILE1018	4.65093				
Sm35					
ARG841	2.69201	Hydrogen Bond	Conventional Hydrogen Bond	512.92	-7.7
LYS745	2.85561		Carbon Hydrogen Bond		
LEU718	3.50013				
ASP855	3.76702				
CYS797	4.42943	Other	Pi-Sulfur		
PHE723	3.75207	Hydrophobic	Pi-Pi Stacked		
ALA722	4.95906		Pi-Alkyl		
Sm36					
ASP855	2.45387	Hydrogen Bond	Conventional Hydrogen Bond	522.64	-8.3
THR854	2.41559		Carbon Hydrogen Bond		
CYS797	2.15071				
ASP800	3.51336				
LEU718	3.88883	Hydrophobic	Pi-Sigma		
MET790	5.9436	Other	Pi-Sulfur		
	5.14002	Hydrophobic	Pi-Pi T-shaped		
VAL726	5.32233		Pi-Alkyl		
LEU718	5.18966				
VAL726	4.52131				
LEU844	5.30615				
VAL726	5.42634				
ALA743	4.11649				
LEU844	4.81863				
Sm39					

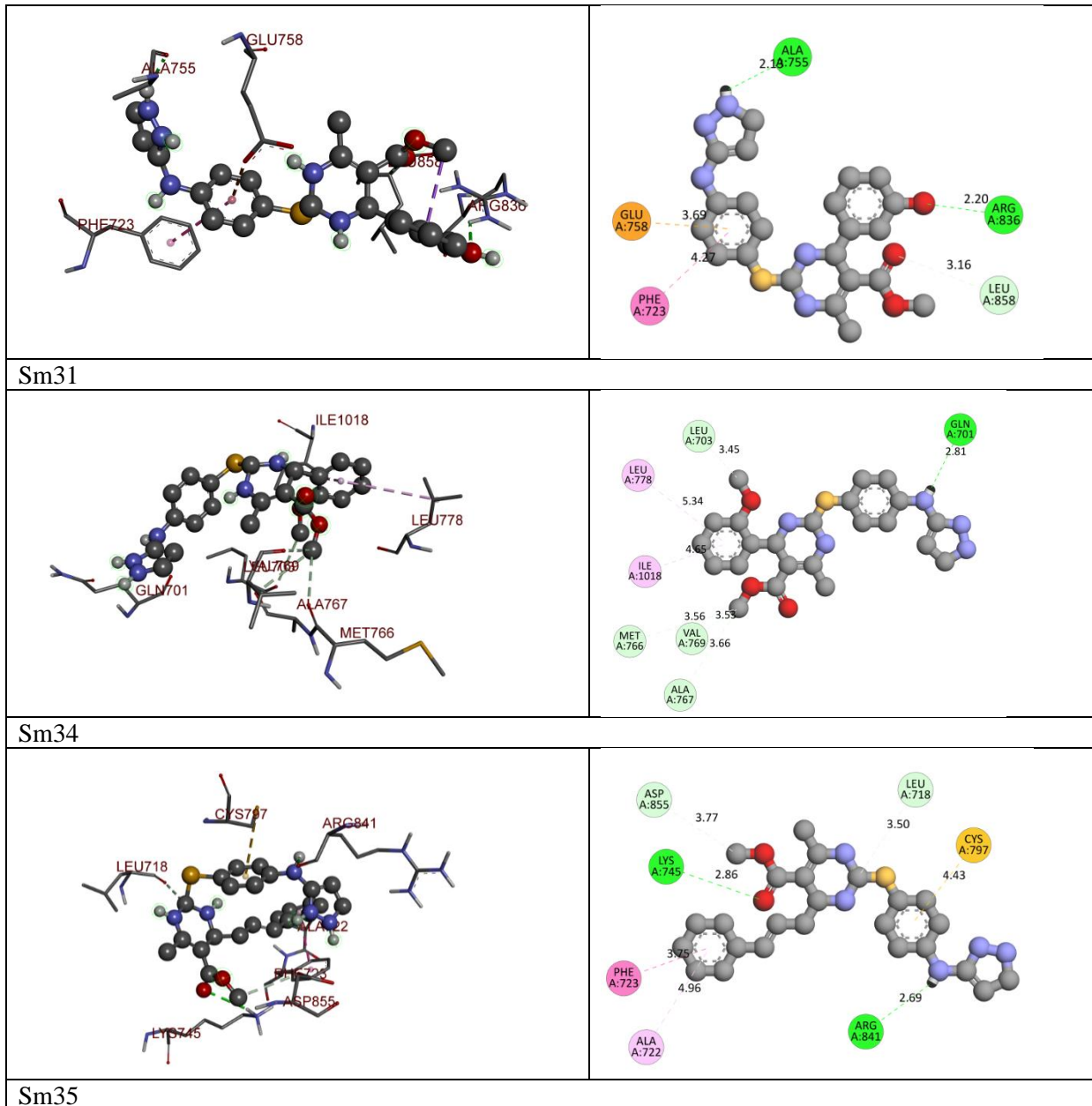
ASP837	1.89584	Hydrogen Bond	Conventional Hydrogen Bond	517.84	-7.6
ASN842	1.93995		Carbon Hydrogen Bond		
ARG841	3.79636		Pi-Sigma		
	3.85823	Hydrophobic	Pi-Pi Stacked		
PHE723	3.83019		Pi-Alkyl		
VAL726	4.1485				

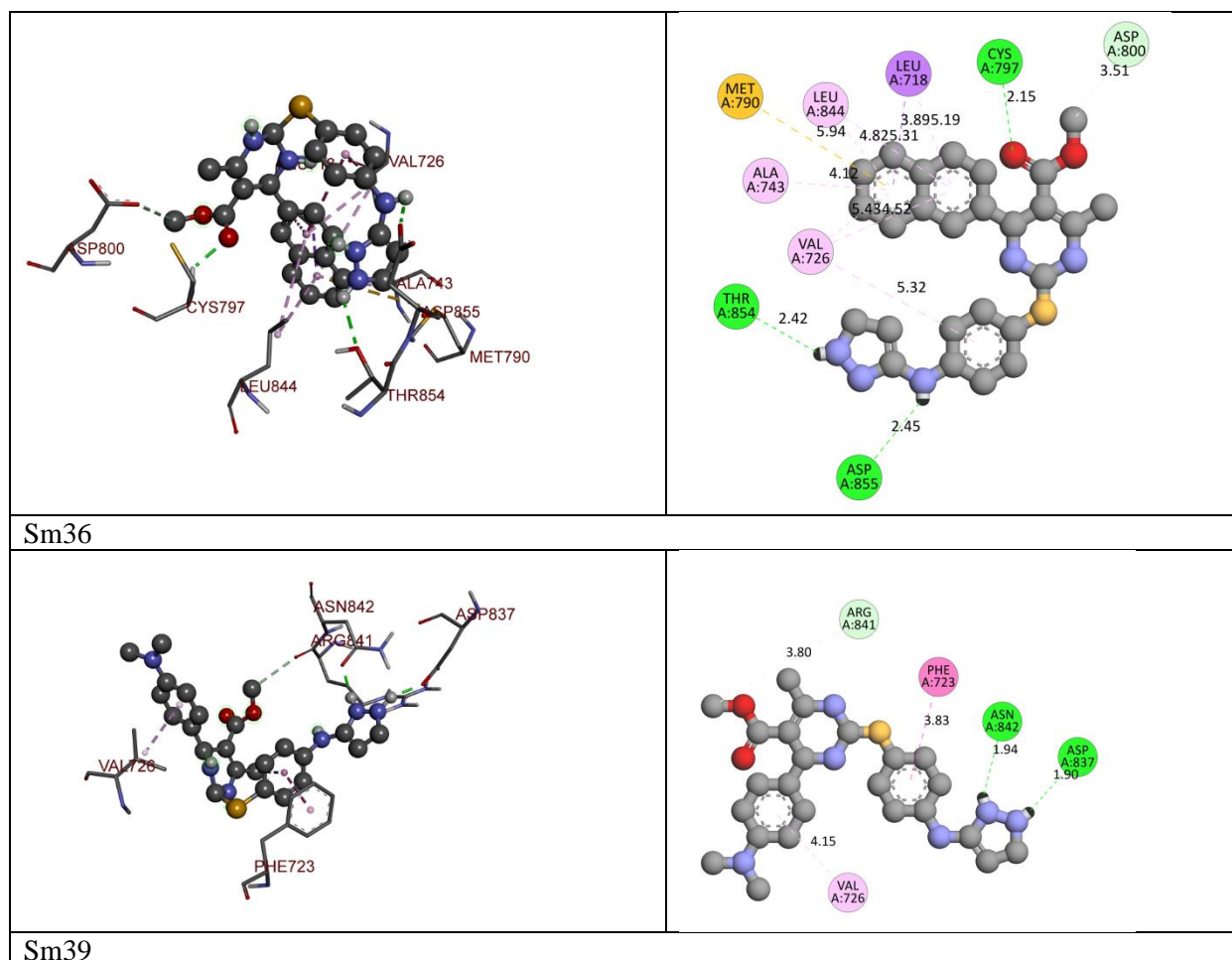
Table 6. The 3D- and 2D-docking poses of the molecules

3D-docking poses	2D-docking poses
	
Native ligand	
	
Sm21	
	
Sm22	

<p>Sm23</p>	
<p>Sm25</p>	
<p>Sm26</p>	

	
<p>Sm27</p>	
	
<p>Sm28</p>	
	
<p>Sm29</p>	





In present study we have designed and developed some methyl 2-(4-(1H-pyrazol-5-ylamino) phenylthio)-1,2,3,4-tetrahydro-6- methylpyrimidine-5-carboxylatederivativesas potential EGFR inhibitors. In accordance with Lipinski's and Veber's rule (Table 2). The log P values of all the molecules were between the ranges 1.39 to 4.43 which indicates optimum lipophilicity. Lipophilicity is a significant feature of the molecule that affects how it works in the body[18]. It is determined by the compound's Log P value, which measures the drug's permeability in the body to reach the target tissue[26,27]. The molecular weight of all the molecules was around 500 Da which indicates active better transport of the molecules through biological membrane. Fortunately, the Lipinski rule of 5 had not been compromised by the compounds[14,15]. All the compounds except **sm23**, **sm24**, **sm32**, **sm37** and **sm40** violated theLipinski rule of 5 .The total polar surface area (TPSA) and the number of rotatable bonds have been found to better discriminate between compounds that are orally active or not. According to Veber's rule, TPSA should be ≤ 140 and number of rotatable bonds should be ≤ 10 . It was observed that, compound **sm37**violated the Veber's rule, as it has TPSA 215\AA^2 .

In order to further optimize the compounds, pharmacokinetics and drug-likeness properties were calculated for each one. All the compounds showed no penetration to the blood-brain barrier (BBB). The log K_p (skin penetration, cm/s) and bioavailability values of all the compounds were within acceptable

limits. (Table 3).The GI absorption of all the compounds was found to be high except for **sm30**, **sm32**, **sm33**, **sm37**, **sm38** and **sm40**.

In acute toxicity predictions, class-III i.e. toxic if swallowed ($50 < LD_{50} \leq 300$), toxicity class-IV which means harmful if swallowed ($300 < LD_{50} \leq 2000$), class-V which indicate may be harmful if swallowed ($2000 < LD_{50} \leq 5000$)[21]. From this virtual screening, it was concluded that all the compounds fall in class IV, V & VI of toxicity, which means they possess drug-like properties and hence were subjected to molecular docking studies. Out of 20 screened molecules through ADMET analysis, compounds **sm37** displayed low absorption and toxicity class-II therefore eliminated from further screening (Table 4). The binding affinities of the derivatives have been compared with the binding mode of native ligand present in the crystal structure of EGFR enzyme (PDB ID: 5Y9T).

Native ligand (naquotinib) displayed -8.3 kcal/mol binding affinity with EGFR and formed three conventional and one carbon-hydrogen bond with Gly857, Glu762, and Glu758. It has developed electrostatic (Pi-anion, attractive charge) and hydrophobic bonds (alkyl and Pi-alkyl) with Glu758, Glu762, Ala755, Pro877, and Leu858. All the designed molecules displayed most potent interactions than the native ligand. Many derivatives exhibited more than two hydrogen bonds with the target. The compounds which have formed three or more hydrogen bonds have been selected for the synthesis and biological activity. The formation of hydrogen bonds with target can effectively modulate the activity of enzyme and exhibit potent pharmacological response. There are many compounds which exhibited more binding affinity but did not formed more than three hydrogen bonds, in that case some more derivatives selected for the synthesis. The compound **sm21**, **sm22**, **sm23**, **sm24**, **sm25**, **sm26**, **sm27**, **sm28**, **sm29**, **sm31**, **sm34**, **sm35**, **sm36** and **sm39** have been selected as most potent molecules from virtual screening.

The compound **sm21** exhibited -8.8 kcal/mol of binding affinity and formed six conventional hydrogen bonds with Leu777, Ala1013, Tyr1016, Asn700; Gln701 & Arg776. It has developed one electrostatic (Pi-cation) interactions with Arg776. The compound **sm22** exhibited -7.3 kcal/mol of binding affinity and formed two conventional hydrogen bonds with Asp837 & Asn842. It has developed two hydrophobic (Pi-sigma & pi-pi stacked) interactions with Val726 & Phe723. The compound **sm23** exhibited -8.9 kcal/mol of binding affinity and formed seven conventional hydrogen bonds with Leu718, Arg841, Asp855, and Thr854 & Glu762. It has developed two hydrophobic (Pi-sigma & pi-alkyl) interactions with Val726 & Phe723. It also displayed one electrostatic (pi-anion) interaction with Asp855. The compound **sm24** exhibited -8.5 kcal/mol of binding affinity and formed four conventional hydrogen bonds with Leu718, Phe795 & Asp800. It has developed two hydrophobic (Pi-sigma) bonds with Leu718 & Leu844. It also displayed hydrophobic interactions (pi-pi T shaped, alkyl, pi-alkyl) with Leu718, Ala743, Leu844 & Val726.

The compound **sm25** exhibited -8.3 kcal/mol of binding affinity and formed three conventional hydrogen bonds with Leu718, Asp837, Asn842. It also showed two carbon hydrogen bonds with Arg841 & Asp855. It has developed two hydrophobic (Pi-sigma, pi-pi stacked & pi-alkyl) interactions with Val726, Phe723, Leu718, Ala743 & Leu844. The compound **sm26** showed -8.5 kcal/mol of binding affinity and formed four conventional hydrogen bonds with Leu718, Phe795 & Asp800. It also showed two carbon hydrogen bonds with Arg841 & Asp855. It has developed two hydrophobic (Pi-sigma, pi-pi stacked, alkyl & pi-alkyl) interactions with Leu718, Leu844, Ala743 & Leu844. The compound **sm27** exhibited -8.3 kcal/mol of binding affinity and formed three conventional hydrogen bonds with Ala1013; Tyr1016 & Leu703. It has developed one hydrophobic (pi-alkyl) interactions with Ile1018. The compound **sm28** showed -8.8 kcal/mol of binding affinity and formed six conventional hydrogen bonds with Ala767, Leu778, Ala1013, Tyr1016; Leu703 & Arg831. It has developed two hydrophobic (pi-alkyl) interactions with Ala743 & Ile1018. The compound **sm29** showed -8.6 kcal/mol of binding affinity and formed five conventional hydrogen bonds with Asp855, Asp837, Asn842, and Thr854. It also showed one carbon

hydrogen bond with Gly796. It has developed two hydrophobic (pi-pi T-shaped & pi-alkyl) interactions with Phe723 & Leu844.

The compound **sm31** showed -7.3 kcal/mol of binding affinity and formed two conventional hydrogen bonds with Ala755 & Arg836. It also exhibited one carbon hydrogen bond with Leu858. It has developed two hydrophobic (Pi-sigma, pi-pi stacked) interactions with Phe723. The compound **sm34** showed -7.7 kcal/mol of binding affinity and formed one conventional hydrogen bond with Gln701 & four carbon hydrogen bonds with Leu703, Met766, and Ala767 & Val769. It has developed two hydrophobic (p-alkyl) interactions with Leu778 & Ile1018. The compound **sm35** displayed -7.7 kcal/mol of binding affinity and formed two conventional hydrogen bonds with Arg841 & Lys745 & two carbon hydrogen bonds with Leu718 & Asp855. It has developed two hydrophobic (Pi-Pi Stacked, pi-alkyl) interactions with Phe723 & Ala722. The compound **sm36** displayed -8.3 kcal/mol of binding affinity and formed three conventional hydrogen bonds with Asp855, Thr854 & Cys797 also one carbon hydrogen bonds with Asp800. It has developed hydrophobic (Pi-Pi Stacked, pi-sigma, pi-sulfur, pi-pi-T shaped, pi-alkyl) interactions with Leu718, Val726, Leu844, & Ala743. The compound **sm39** showed -7.6 kcal/mol of binding affinity and formed two conventional hydrogen bonds with Asp837, Asn842 & one carbon hydrogen bond with Arg841. It has developed three hydrophobic (Pi-Pi Stacked, pi-sigma, p-alkyl) interactions with Phe723 & Val726.

4. Conclusion

A lot of *in silico* models are developed for prediction of chemical ADMET properties. However, it is still not easy to evaluate the drug-likeness of compounds in terms of so many ADMET properties. In present study, we have designed some methyl 2-(4-(1H-pyrazol-5-ylamino) phenylthio)-1,2,3,4-tetrahydro-6-methylpyrimidine-5-carboxylatederivatives to be developed as potential EGFR inhibitors for the treatment of cancer. The designed derivatives were screened through Lipinski rule, Veber's rule, ADMET analysis, drug-likeness properties and molecular docking. From above screening it was observed that native ligand formed three conventional hydrogen bonds and exhibited -8.3 kcal/mol binding affinity therefore, the molecules which formed three or more conventional hydrogen bonds and exhibited >8.3 kcal/mol binding affinity with enzyme are considered as most potent and selected for wet lab synthesis followed by biological evaluation. Molecules **sm21**, **sm23**, **sm24**, **sm25**, **sm26**, **sm27**, **sm28**, **sm29**, and **sm36** had formed either three or more conventional hydrogen bonds with EGFR enzyme and hence selected for synthesis.

Acknowledgments

The authors are thankful to Dr. P. Y. Pawar, Principal of Dr. Vitthalrao Vikhe patil foundation's, College of Pharmacy, Vilad Ghat, Ahmednagar for providing the necessary facilities to carry out the research work. Furthermore, authors are also thankful to the people who directly and indirectly help me to carry out this research work.

References

1. Chan, D.L.H.; Segelov, E.; Wong, R.S.H.; Smith, A.; Herbertson, R.A.; Li, B.T.; Tebbutt, N.; Price, T.; Pavlakis, N. Epidermal Growth Factor Receptor (EGFR) Inhibitors for Metastatic Colorectal Cancer. *Cochrane Database Syst. Rev.* 2017, 2017.
2. Grünwald, V.; Hidalgo, M. Developing Inhibitors of the Epidermal Growth Factor Receptor for Cancer Treatment. *J. Natl. Cancer Inst.* 2003, 95, 851–867.
3. Song, Z.; Ge, Y.; Wang, C.; Huang, S.; Shu, X.; Liu, K.; Zhou, Y.; Ma, X. Challenges and Perspectives on the Development of Small-Molecule EGFR Inhibitors against T790M-Mediated Resistance in Non-Small-Cell Lung Cancer: Miniperspective. *J. Med. Chem.* 2016, 59, 6580–6594, doi:10.1021/acs.jmedchem.5b00840.
4. Harari, P.M. Epidermal Growth Factor Receptor Inhibition Strategies in Oncology. *Endocr.*

- Relat. Cancer* 2004, *11*, 689–708.
5. Woodburn, J.R. The Epidermal Growth Factor Receptor and Its Inhibition in Cancer Therapy. In *Proceedings of the Pharmacology and Therapeutics*; 1999; Vol. 82, pp. 241–250.
 6. Chen, L.; Fu, W.; Zheng, L.; Liu, Z.; Liang, G. Recent Progress of Small-Molecule Epidermal Growth Factor Receptor (EGFR) Inhibitors against C797S Resistance in Non-Small-Cell Lung Cancer. *J. Med. Chem.* 2018, *61*, 4290–4300.
 7. Attili, I.; Karachaliou, N.; Conte, P.F.; Bonanno, L.; Rosell, R. Therapeutic Approaches for T790M Mutation Positive Non-Small-Cell Lung Cancer. *Expert Rev. Anticancer Ther.* **2018**, *18*, 1021–1030, doi:10.1080/14737140.2018.1508347.
 8. Ai, X.; Guo, X.; Wang, J.; Stancu, A.L.; Joslin, P.M.N.; Zhang, D.; Zhu, S. Targeted Therapies for Advanced Non-Small Cell Lung Cancer. *Oncotarget* **2018**, *9*, 37589–37607, doi:10.18632/oncotarget.26428.
 9. Bryce, A.H.; Rao, R.; Sarkaria, J.; Reid, J.M.; Qi, Y.; Qin, R.; James, C.D.; Jenkins, R.B.; Boni, J.; Erlichman, C.; et al. Phase I Study of Temsirolimus in Combination with EKB-569 in Patients with Advanced Solid Tumors. *Invest. New Drugs* **2012**, *30*, 1934–1941, doi:10.1007/s10637-011-9742-1.
 10. Grünwald, V.; Hidalgo, M. Developing Inhibitors of the Epidermal Growth Factor Receptor for Cancer Treatment. *J. Natl. Cancer Inst.* **2003**, *95*, 851–867, doi:10.1093/jnci/95.12.851.
 11. Roskoski, R. Cyclin-Dependent Protein Kinase Inhibitors Including Palbociclib as Anticancer Drugs. *Pharmacol. Res.* **2016**, *107*, 249–275, doi:10.1016/j.phrs.2016.03.012.
 12. Khan, S.L.; Siddiqui, F.A.; Shaikh, M.S.; Nema, N. V.; Shaikh, A.A. Discovery of Potential Inhibitors of the Receptor-Binding Domain (RBD) of Pandemic Disease-Causing SARS-CoV-2 Spike Glycoprotein from Triphala through Molecular Docking. *Curr. Chinese Chem.* **2021**, *01*, doi:10.2174/2666001601666210322121802.
 13. Siddiqui, F.A.; Khan, S.L.; Marathe, R.P.; Nema, N. V. Design, Synthesis, and In Silico Studies of Novel N-(2-Aminophenyl)-2,3-Diphenylquinoxaline-6-Sulfonamide Derivatives Targeting Receptor-Binding Domain (RBD) of SARS-CoV-2 Spike Glycoprotein and Their Evaluation as Antimicrobial and Antimalarial Agents. *Lett. Drug Des. Discov.* **2021**, *18*, 915–931, doi:10.2174/1570180818666210427095203.
 14. Khan, A.; Unnisa, A.; Sohel, M.; Date, M.; Panpaliya, N.; Saboo, S.G.; Siddiqui, F.; Khan, S. Investigation of Phytoconstituents of *Enicostemma Littorale* as Potential Glucokinase Activators through Molecular Docking for the Treatment of Type 2 Diabetes Mellitus. *Silico Pharmacol.* **2022**, *10*, doi:10.1007/s40203-021-00116-8.
 15. Shntaif, A.H.; Khan, S.; Tapadiya, G.; Chettupalli, A.; Saboo, S.; Shaikh, M.S.; Siddiqui, F.; Amara, R.R. Rational Drug Design, Synthesis, and Biological Evaluation of Novel N-(2-Arylamino-phenyl)-2,3-Diphenylquinoxaline-6-Sulfonamides as Potential Antimalarial, Antifungal, and Antibacterial Agents. *Digit. Chinese Med.* **2021**, *4*, 290–304, doi:10.1016/j.dcm.2021.12.004.
 16. Khan, Sharuk L.; Siddiqui, F.A. Beta-Sitosterol: As Immunostimulant, Antioxidant and Inhibitor of SARS-CoV-2 Spike Glycoprotein. *Arch. Pharmacol. Ther.* **2020**, *2*, doi:10.33696/pharmacol.2.014.
 17. Chaudhari, R.N.; Khan, S.L.; Chaudhary, R.S.; Jain, S.P.; Siddiqui, F.A. B-Sitosterol: Isolation from *Muntingia Calabura* Linn Bark Extract, Structural Elucidation And Molecular Docking Studies As Potential Inhibitor of SARS-CoV-2 Mpro (COVID-19). *Asian J. Pharm. Clin. Res.* **2020**, *13*, 204–209, doi:10.22159/ajpcr.2020.v13i5.37909.
 18. Khan, S.; Kale, M.; Siddiqui, F.; Nema, N. Novel Pyrimidine-Benzimidazole Hybrids with

- Antibacterial and Antifungal Properties and Potential Inhibition of SARS-CoV-2 Main Protease and Spike Glycoprotein. *Digit. Chinese Med.***2021**, 4, 102–119, doi:10.1016/j.dcm.2021.06.004.
19. Khan, S.L.; Sonwane, G.M.; Siddiqui, F.A.; Jain, S.P.; Kale, M.A.; Borkar, V.S. Discovery of Naturally Occurring Flavonoids as Human Cytochrome P450 (CYP3A4) Inhibitors with the Aid of Computational Chemistry. *Indo Glob. J. Pharm. Sci.***2020**, 10, 58–69, doi:10.35652/igjps.2020.10409.
 20. Daina, A.; Michielin, O.; Zoete, V. SwissADME: A Free Web Tool to Evaluate Pharmacokinetics, Drug-Likeness and Medicinal Chemistry Friendliness of Small Molecules. *Sci. Rep.***2017**, 7, doi:10.1038/srep42717.
 21. Banerjee, P.; Eckert, A.O.; Schrey, A.K.; Preissner, R. ProTox-II: A Webserver for the Prediction of Toxicity of Chemicals. *Nucleic Acids Res.***2018**, 46, W257–W263, doi:10.1093/nar/gky318.
 22. Dallakyan, S.; Olson, A.J. Small-Molecule Library Screening by Docking with PyRx. *Methods Mol. Biol.***2015**, 1263, 243–250, doi:10.1007/978-1-4939-2269-7_19.
 23. Rappé, A.K.; Casewit, C.J.; Colwell, K.S.; Goddard, W.A.; Skiff, W.M. UFF, a Full Periodic Table Force Field for Molecular Mechanics and Molecular Dynamics Simulations. *J. Am. Chem. Soc.***1992**, 114, 10024–10035, doi:10.1021/ja00051a040.
 24. San Diego: Accelrys Software Inc. Discovery Studio Modeling Environment, Release 3.5. *Accelrys Softw. Inc.***2012**.
 25. Khan, S.L.; Siddiqui, F.A.; Jain, S.P.; Sonwane, G.M. Discovery of Potential Inhibitors of SARS-CoV-2 (COVID-19) Main Protease (Mpro) from Nigella Sativa (Black Seed) by Molecular Docking Study. *Coronaviruses***2020**, 2, 384–402, doi:10.2174/2666796701999200921094103.
 26. Krzywinski, M.; Altman, N. Points of Significance: Significance, P Values and t-Tests. *Nat. Methods***2013**, 10, 1041–1042, doi:10.1038/nmeth.2698.
 27. Lipinski, C.A.; Lombardo, F.; Dominy, B.W.; Feeney, P.J. Experimental and Computational Approaches to Estimate Solubility and Permeability in Drug Discovery and Development Settings. *Adv. Drug Deliv. Rev.* 2012, 64, 4–17.